9 May 2008 | $10

Science

AAAS

Volume 320, Issue 5877

COVER

Lake Boku at the Ounianga oasis in remote northeastern Chad, one of the few remaining bodies of water in the almost rainless Sahara. Still sustained by fossil groundwater dating from the humid past, it is doomed because of encroaching dunes. See page 765.

Photo: S. Kröpelin

DEPARTMENTS

EDITORIAL

NEWS OF THE WEEK

NEWS FOCUS

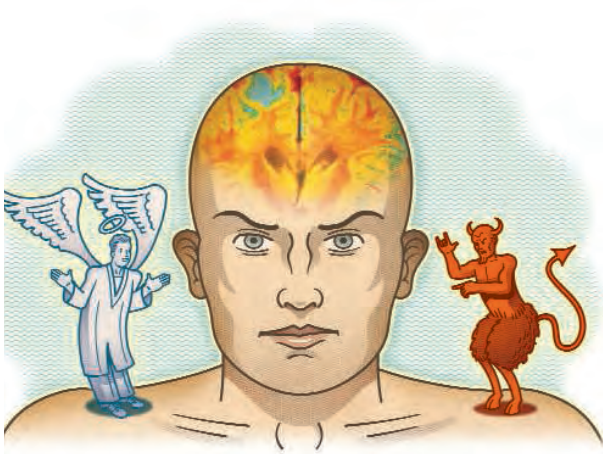

734

LETTERS

BOOKS *ET AL.*

748

POLICY FORUM

PERSPECTIVES

CONTENTS continued >>

Published by AAAS

Climate-Driven Ecosystem Succession in the Sahara: The Past 6000 Years

S. Kröpelin,[1]* D. Verschuren,[2] A.-M. Lézine,[3] H. Eggermont,[2] C. Cocquyt,[2,4] P. Francus,[5,6] J.-P. Cazet,[3] M. Fagot,[2] B. Rumes,[2] J. M. Russell,[7] F. Darius,[1] D. J. Conley,[8] M. Schuster,[9] H. von Suchodoletz,[10,11] D. R. Engstrom[12]

Desiccation of the Sahara since the middle Holocene has eradicated all but a few natural archives recording its transition from a "green Sahara" to the present hyperarid desert. Our continuous 6000-year paleoenvironmental reconstruction from northern Chad shows progressive drying of the regional terrestrial ecosystem in response to weakening insolation forcing of the African monsoon and abrupt hydrological change in the local aquatic ecosystem controlled by site-specific thresholds. Strong reductions in tropical trees and then Sahelian grassland cover allowed large-scale dust mobilization from 4300 calendar years before the present (cal yr B.P.). Today's desert ecosystem and regional wind regime were established around 2700 cal yr B.P. This gradual rather than abrupt termination of the African Humid Period in the eastern Sahara suggests a relatively weak biogeophysical feedback on climate.

One of the most prominent environmental changes of the past 10,000 years is the transition of northern Africa from a "green Sahara" (*1*) during the early Holocene "African Humid Period" (*2*) to the world's largest warm desert today. Detailed knowledge of the tempo and mode of this transition is crucial for understanding the interaction between tropical and mid-latitude weather systems (*3*–*6*) and the multiple impacts of mineral aerosols exported from the Sahara on global climate (*7*–*10*) and distant ecosystems (*11*–*13*). The distinct lack of high-quality paleoenvironmental records covering the past four to five millennia from within the Sahara desert (*14*) (SOM text 1) has directed substantial effort to the modeling of African monsoon dynamics in response to orbital insolation changes (e.g., *15*, *16*), and of the influence of surface temperature changes in the adjacent tropical ocean (e.g., *4*) and biogeophysical feedbacks between climate and vegetation (*1*, *17*–*20*). Modeling results suggest that a strong positive biogeophysical feedback between rainfall and vegetation (*18*) appear to be supported by the record of terrigenous (land-eroded) dust deposited in deep-sea sediments downwind from the Sahara, which shows a sudden increase at 5500 calendar years before the present (cal yr B.P.) (*2*, *21*). As a result, the Holocene drying of the Sahara (i.e., termination of the "African Humid Period") is widely believed to have been an abrupt event, completed within a few hundred years (e.g., *22*, *23*). In turn, this abrupt event of possible continental scale is regarded as a prime example of catastrophic regime shifts in natural ecosystems (e.g., *24*, *25*).

In this context, we present a continuous and accurately dated paleo-environmental record covering the past 6000 years from within the Sahara, using multiple proxies and indicators preserved in a finely laminated lake-sediment sequence from northern Chad. High-resolution sedimentological and geochemical data coupled with biological indicators (pollen, spores, and the remains of aquatic biota) permit a precise reconstruction of terrestrial and aquatic ecosystem response to climate-driven moisture-balance changes in the now hyperarid core of the east-central Sahara desert.

Study site and material. Lake Yoa is one of a handful of permanent lakes occupying Pleistocene deflation basins in Ounianga, situated halfway between the Tibesti and Ennedi mountains (Fig. 1). The subtropical desert climate of this area is characterized by high daytime temperatures, negligible rainfall, and dry northeasterly trade winds blowing almost year-round through the Tibesti-Ennedi corridor (Fig. 1C) (SOM text 2). The Ounianga lakes are maintained against this extremely negative water balance by groundwater inflow from the Nubian Sandstone Aquifer, which was last recharged during the early Holocene (*26*). This stable groundwater input ensured permanence of the aquatic ecosystem throughout the dry late-Holocene period but dampened its hydrological sensitivity to climate. Sediments in Lake Yoa are finely laminated throughout the sampled upper 7.47 m of the sequence (*27*). Sections with annual lamination (varves) (Fig. 2D) show an average sedimentation rate of 1.3 mm per year, in support of the age-depth model constructed from 12 accelerator mass spectrometry radiocarbon dates and the 1964 caesium marker of nuclear bomb testing (*27*) (table S1).

The Lake Yoa record documents dramatic changes through time in three important components of the Saharan paleoenvironment. First, it traces the evolution of the local aquatic ecosystem from a dilute freshwater habitat to the present-day hypersaline oasis. Second, it reveals the establishment of today's terrestrial desert ecosystem as the result of continuous vegetation succession between 5600 and 2700 cal yr B.P. Third, it shows the changing regional wind regime, culminating in establishment of today's almost year-round northeasterly winds around 2700 cal yr B.P.

Evolution of the aquatic ecosystem. The most prominent feature in the recorded history of Lake Yoa is its relatively rapid transition, between 4200 and 3900 cal yr B.P., from a seemingly stable freshwater habitat (surface-water conductivity of 300 to 500 µS/cm) to a true salt lake (>10,000 µS/cm) in which only specialized fauna and flora can survive (Fig. 2A and figs. S2 to S4) (*27*). In reality, the ecology of Lake Yoa evolved continuously during the past 6000 years, in response to changes in water chemistry, nutrient dynamics, and substrate availability driven by changing lake hydrology and water balance (SOM text 3 and 4). In brief, organic matter deposition (Fig. 2C) (SOM text 5) and the stratigraphy of phytoplankton species (figs. S2 and S3) indicate that Lake Yoa switched from a less to a more productive aquatic ecosystem ~5600 cal yr B.P. Lake productivity remained high after the fresh-to-saline transition until ~3300 cal yr B.P., when conductivity rose above 20,000 µS/cm (Fig. 2A), and also the most salt-tolerant freshwater biota disappeared (fig. S4). From that moment on, both primary productivity (percentage organic matter) (Fig. 2C) and secondary productivity (represented by fossil chironomid abundance) (fig. S4) gradually declined, until by 2700 cal yr B.P. they stabilized at ~50 to 70% lower values. This transition coincided with a virtually complete collapse of the Lake Yoa diatom flora [biogenic SiO_2 (Fig. 2B); diatom cell counts (fig. S3)]. This fairly unproductive, hypersaline aquatic ecosystem then acquired its modern-day biology with establishment of the

[1]Africa Research Unit, Institute of Prehistoric Archaeology, University of Cologne, Jennerstraße 8, D-50823 Köln, Germany. [2]Limnology Unit, Department of Biology, Ghent University, K. L. Ledeganckstraat 35, B-9000 Gent, Belgium. [3]Laboratoire des Sciences du Climat et de l'Environnement, CNRS-CEA-UVSQ UMR 1572, L'Orme des Merisiers, F-91191 Gif-Sur-Yvette, France. [4]National Botanic Garden of Belgium, Domein van Bouchout, B-1860 Meise, Belgium. [5]Institut National de la Recherche Scientifique, Centre Eau, Terre et Environnement, 490 Rue de la Couronne, Québec, Québec G1K 9A9, Canada. [6]GEOTOP, Geochemistry and Geodynamics Research Centre, C.P. 8888, Université du Québec à Montréal, Succursale, Centre-Ville, Montréal, Québec H3C 3P8, Canada. [7]Geological Sciences, Brown University, Box 1846, Providence, RI 02912, USA. [8]GeoBiosphere Centre, Department of Geology, Lund University, Sölvegatan 12, SE-22362 Lund, Sweden. [9]Institut International de Paléoprimatologie, Paléontologie Humaine, Evolution et Paléoenvironnements, CNRS UMR 6046, Université de Poitiers, 40 Avenue du Recteur Pineau, F-86022 Poitiers, France. [10]Geoforschungszentrum Potsdam, Telegrafenberg, D-14473 Potsdam, Germany. [11]Lehrstuhl für Geomorphologie, Universität Bayreuth, Universitätsstraße 30, D-95440 Bayreuth, Germany. [12]St. Croix Watershed Research Station, Science Museum of Minnesota, Marine on St. Croix, MN 55047, USA.

*To whom correspondence should be addressed. E-mail: s.kroe@uni-koeln.de

salt-loving hemipteran *Anisops* as the dominant macrozooplankton species ~2700 cal yr B.P. and appearance of brine flies (*Ephydra*) ~1500 cal yr B.P. (fig. S2).

Evolution of the terrestrial ecosystem. Palynological and lithological indicators describe a more progressive evolution of the terrestrial ecosystem surrounding Lake Yoa. Throughout the last 6000 years, the regional vegetation was dominated by grasses (Poaceae), in association with scattered *Acacia* trees (Fig. 2G). Before 4300 cal yr B.P. the regional landscape was an open grass savannah complemented with modest but indicative populations of tropical (Sudanian) trees (e.g., *Piliostigma*, *Lannea*, and *Fluggea virosa*), which today commonly occur in wooded grasslands and dry forests at least 300 km to the south. Their co-occurrence with ferns (Fig. 2G) suggests that these trees formed streambank communities in temporarily flooded river valleys (wadis). The savannah also included tropical herb species (e.g., *Mitracarpus* and *Spermacoce*). This mid-Holocene pollen assemblage was completed by the mountain shrub *Erica arborea*, now restricted to a few small areas above 2900 m altitude in the Tibesti. Substantial input of *Erica* pollen throughout the period with abundant humid plant indicators may suggest that a river from the Tibesti flowed at least seasonally into Lake Yoa until ~4300 cal yr B.P. Drying of this exotic river may have partly accounted for the negative water balance that terminated the lake's freshwater ecosystem shortly thereafter. The first evidence of ecosystem drying in the Ounianga region, however, is already observed at 5600 cal yr B.P., with increasing *Acacia* and the expansion of plants typifying semidesert environments (e.g., *Boerhavia* and *Tribulus*). The demise of tropical trees, accelerating after 4800 cal yr B.P., was initially compensated by expansion of Sahel-type trees and shrubs (e.g., *Commiphora* and *Balanites*), of which the northern limit today does not extend beyond the Ennedi (Fig. 1C). This Sahelian vegetation component, although substantive, was relatively short-lived, because by ~4300 cal yr B.P. *Commiphora* dwindled to a sporadic occurrence.

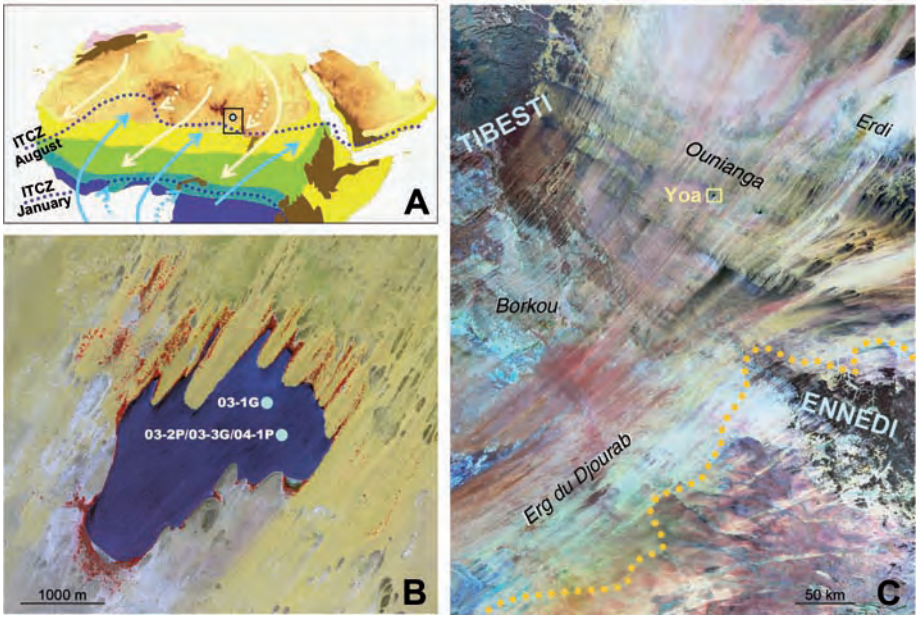

Fig. 1. Location of Lake Yoa [19.03° N, 20.31° E, 380 m above sea level (asl)] at continental and regional scales. (**A**) Map of Africa north of the equator highlighting land >1000 m asl, the natural distribution of vegetation zones (*29*), and synoptic climatology. Arrows: moist tropical Atlantic monsoon circulation (blue) and dry northeasterly trades (light yellow) in relation to the position of the Intertropical Convergence Zone (ITCZ) during Northern Hemisphere summer and winter [adapted from (*9*)]. Vegetation zones, from north to south: Mediterranean evergreen forest (pink), Mediterranean scrubland (light yellow), desert (ochre, with relief), Sahelian wooded grassland (yellow), Sudanian wooded grassland (green), tropical dry forest (blue-green), and tropical rainforest (dark blue); mountain ranges are shown in dark brown. (**B**) Quickbird satellite image of Lake Yoa (4.3 km^2, 26 m deep), bounded to the south and west by sandstone cliffs and to the north and east by dunes of quartz sand. These accumulate in low-wind zones beneath the dissected rim of the Ounianga escarpment, and their progressive migration into the lake has now reached its modern depositional center. *Typha* (cattail) stands develop near groundwater inflow along the northern and eastern lakeshore. Also shown are the locations of sediment cores collected in 2003 and 2004, which together form the studied sediment sequence (*27*). (**C**) Landsat 7 Geocover mosaic satellite image of the Ounianga region showing the main geomorphological features and the northern limit of Sahelian grassland (dotted line) (*28*).

General deterioration of the terrestrial ecosystem of northern Chad ~4800 to 4300 cal yr B.P. is also reflected in a dramatic fall in grass pollen influx, which we interpret to indicate that grass cover became sparse or discontinuous at the landscape scale (despite grass still contributing ~50 to 55% to the pollen sum) (Fig. 2G). This observation is confirmed by the rise in magnetic susceptibility above background values of 2 to 10 $\times 10^{-6}$ SI units from 4300 cal yr B.P., reflecting increased input of wind-blown dust (Fig. 2E) (*27* and SOM text 6). The gradual rise of fine sand (75 to 150 μm) in the upper half of the sequence, above background values of 1 to 5% (Fig. 2F), indicates that from 3700 cal yr B.P. onward, winds also increasingly entrained sand. A first (semi-)desert plant community developed between 3900 and 3100 cal yr B.P. with expansion of herbs such as *Blepharis*, *Boerhavia* (Fig. 2G) and *Tribulus* (scarce), followed at ~2700 cal B.P. by vegetation found today both in the immediate vicinity of Ounianga and throughout the central Sahara (*28*): *Artemisia*, *Cornulaca*, and Amaranthaceae-Chenopodiaceae, with scattered *Salvadora persica* and *Ephedra* trees (Saharan plant taxa, Fig. 2G), as well as *Acacia*.

The near-synchronous immigration of true desert plant types at ~2700 cal yr B.P. is associated with a marked increase in the influx of grass pollen (Fig. 2G), despite our inference of a by now mostly barren desert landscape (SOM text 7). This switch coincides with magnetic susceptibility reaching a plateau value of ~40 $\times 10^{-6}$ SI units, followed by a modest, gradual decline toward the present (Fig. 2E). We interpret this coincidence to reflect the establishment around 2700 cal yr B.P. of the modern regional wind regime, with strong northeasterly trade winds blowing almost year-round (Fig. 1A). In this interpretation, the greater pollen influx mostly reflects enhanced long-distance transport from a now much expanded pollen source area, including scrubland and steppe at the northern fringe of the Sahara. This interpretation is supported by the occurrence after 2700 cal yr B.P. of pollen from plant species (e.g., *Quercus*) (Fig. 2G) that likely originate from the Mediterranean coast (Fig. 1A) (*29*). The expanded pollen source area implies that average northeasterly wind strength must have increased during this time, either because wintertime trade-wind circulation intensified or because a change in the mean position of the Libyan high-pressure cell now channeled low-level northeasterly flow more effectively through the Tibesti-Ennedi corridor. After passing through the Ounianga region, these surface winds continue into the Bodélé depression of the northern Lake Chad basin, the single most important source of Saharan dust (*9*, *30*). Important topographic control by the Tibesti and Ennedi on the generation of erosive Bodélé low-level jet winds (*31*, *32*) implies that our timing of the onset of the modern wind regime in northeastern Chad

has direct bearing on the history of Saharan dust production and export. We interpret the slightly decreasing dust flux (magnetic susceptibility) at Ounianga since 2700 cal yr B.P. to indicate that deflation during the preceding 1500 years had by that time removed all loose soil laid bare through the loss of vegetation cover (SOM text 6). From that moment on, the mineral dust flux became limited by its rate of erosion from dried-out lake basins and exposed bedrock. Redeposition of sand mobilized in this process led to dune development at the foot of the Ounianga escarpment. The rising sand content after 2700 cal yr B.P. (Fig. 2F) may reflect the gradual migration of these dunes into Lake Yoa (Fig. 1B) and their approach of the midlake coring site.

The record of *Typha* (cattail) pollen (Fig. 2G) illustrates the temporal linkages between the evolution of terrestrial and aquatic ecosystems at Ounianga over the past six millennia.

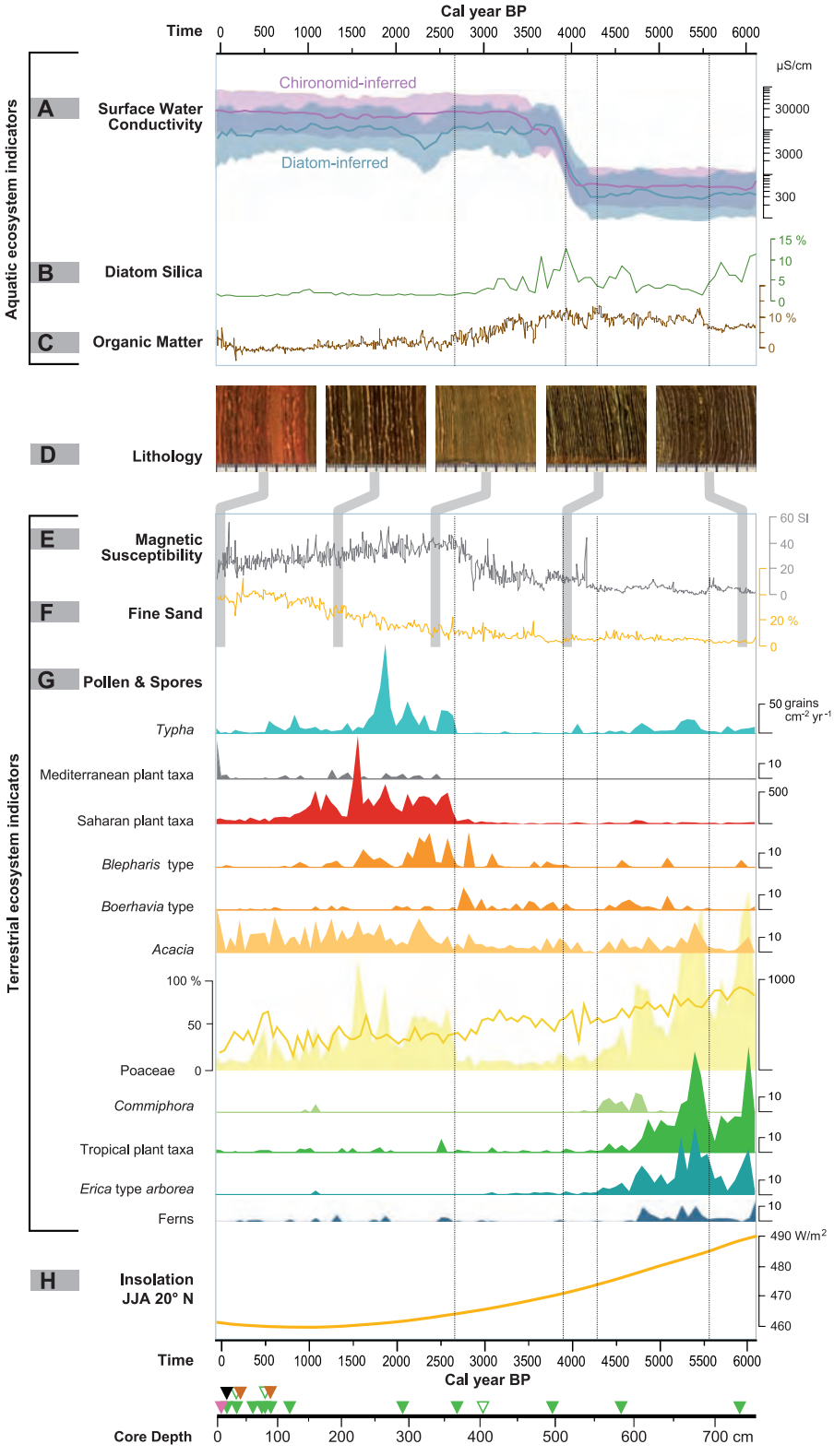

Fig. 2. Evolution of aquatic and terrestrial ecosystem components over the past 6000 years, with episodes of marked change highlighted with stippled vertical lines. The aquatic ecosystem of Lake Yoa is described by paleosalinity reconstructions based on fossil chironomids and diatoms (**A**); and diatom silica in weight percent of SiO_2 (**B**) and bulk organic matter (**C**) as indicators of primary productivity. Core lithology is illustrated by sections of laminated sediment representative for lower, middle, and upper portions of the cored sequence (**D**). The terrestrial ecosystem of the Ounianga region is described by the magnetic susceptibility record of eolian dust input (**E**), the dry-weight fraction of fine sand (**F**), and the influx rate (**G**, right axes) and percentage (G, left axis, Poaceae only) of pollen or spores from principal plant taxa. (**H**) shows local summer insolation over the past 6000 years (*44*). The age-depth model (fig. S1) is constrained by the sediment-water interface (2003 AD), the ^{137}Cs marker of peak nuclear bomb testing (1964 AD, purple) and 17 ^{14}C dates on bulk organic matter (green; open triangles are outliers), with a lake-carbon reservoir correction based on paired ^{14}C dating of bulk organic matter and either charred grass (brown) or 1918 AD in varve years (black) (*27*).

Two episodes of expanded *Typha* swamp occurred at 5500 to 4700 cal yr B.P. and 2700 to 600 cal yr B.P. The first of these coincides with the first recorded evidence for a drying terrestrial ecosystem (Fig. 2G), as well as with indicators of increasing aquatic productivity (Fig. 2C) and community turnover in the phytoplankton (fig. S2). We interpret these data to indicate that by 5600 to 5500 cal yr B.P. climatic deterioration of the regional moisture balance caused parts of the rocky Ounianga plateau to develop drought-tolerant vegetation and forced a lake-level decline that both intensified lake nutrient dynamics and allowed *Typha* swamp to develop along gently sloping shorelines. *Typha* expansion at 2700 cal yr B.P. coincides with the establishment of today's desert plant community and of Lake Yoa as a relatively unproductive, hypersaline desert lake (Fig. 2). We interpret these indicators to signal the stabilization of Lake Yoa at its present elevation, set by the hydrological balance between a hyperarid climate regime, wind-enhanced evaporation, and fossil groundwater input.

Timing and mode of climate change. Arid climatic conditions in the Sahara since ~4300 cal yr B.P. have eradicated all but a few permanent aquatic environments. Paleoenvironmental records covering this period with similar data quality (SOM text 5) are unlikely to exist anywhere else in the arid climate belt of North Africa. Our multiple-indicator reconstruction illustrates the complex relationship between Saharan ecosystems and climate throughout the period of aridification. It gives no indication for abrupt mid-Holocene climate change, or for alternation between marked dry and wet episodes that allowed the vegetation to recover to previous ecological conditions (SOM text 8). Most important, our data do not show an abrupt collapse of the early Holocene terrestrial ecosystem, but a gradual reduction in the abundance of tropical vegetation components followed by loss of grass cover and establishment of the modern desert plant community.

The combined paleoenvironmental evidence indicates that annual rainfall in the Ounianga region was reduced from ~250 mm at 6000 cal yr B.P. to <150 mm by 4300 cal yr B.P., followed by somewhat slower evolution to present-day hyperarid conditions (<50 mm annually) by 2700 cal yr B.P. (SOM text 9). Terrestrial and aquatic ecosystems experienced both gradual evolution and relatively rapid, threshold-type changes, progressing through a predictable sequence of interconnected system responses to climate-driven deterioration of the regional water balance. At the landscape scale this reduction in moisture was effected through decreasing and more intermittent rainfall, lowering of the groundwater table, and the drying out of surface waters. For example, the fairly rapid fresh-to-saline transition of Lake Yoa probably reflects its switch from a hydrologically more open lake system before 4300 cal yr B.P., when substantial surface or subsurface outflow prevented concentration of dissolved salts, to a hydrologically closed system with water output only through evaporation, and a consequent concentration of dissolved salts. The exact timing of this transition depended on a site-specific threshold in the evolving balance between summed inputs (rain, local runoff, groundwater, and river inflow) and outputs (evaporation and subsurface outflow), rather than the timing and rate of regional climate change. Plant community response to climate is also often nonlinear (*25*, *33*), because it is governed by the physiological tolerance of key species to water scarcity and/or osmotic stress (e.g., *34*), by soil moisture thresholds for vegetation persistence, or by the role of vegetation and its spatial patterning in promoting infiltration (*35*) and preventing soil erosion or nutrient loss (*36*, *37*). If mid-Holocene climate change had been concentrated in a relatively short period, the long process of ecological succession and species turnover between "green" and "desert" Sahara states would not have been recorded or would have collapsed into a time window lasting a few centuries rather than the 2.5 millennia observed in our data.

In summary, the Lake Yoa record supports archaeological (*38*) and geological (*14*) data from the eastern Sahara as well as palynological data from the West African Sahel (*39*, *40*) that the iconic record of Saharan dust deposition in the tropical Atlantic Ocean (*2*) is not representative for landscape history throughout dry northern Africa. It is also consistent with climate modeling output (*20*) showing a mostly gradual mid-Holocene precipitation decline over the eastern Sahara (SOM text 8), in line with monsoon-proxy records from elsewhere (*41*–*43*) that indicate a close link between the hydrological cycle in northern subtropical regions and orbital insolation forcing (Fig. 2I). Disagreement with modeling results indicating abrupt mid-Holocene vegetation collapse (*18*, *20*) suggests that the implicated biogeophysical climate-vegetation feedback may have been relatively weak (*6*) and that nonlinear vegetation response to moisture-balance variability superimposed on the long-term drying trend, although certainly affecting individual species distributions, did not lead to abrupt vegetation collapse at the landscape scale.

References and Notes

1. M. Claussen, V. Gayler, *Glob. Ecol. Biogeogr.* **6**, 369 (1997).
2. P. B. deMenocal *et al.*, *Quat. Sci. Rev.* **19**, 347 (2000).
3. COHMAP Members, *Science* **241**, 1043 (1988).
4. J. E. Kutzbach, Z. Liu, *Science* **278**, 440 (1997).
5. A. Ganopolski, C. Kubatzki, M. Claussen, V. Brovkin, V. Petoukhov, *Science* **280**, 1916 (1998).
6. P. Braconnot *et al.*, *Clim. Past* **3**, 279 (2007).
7. A. S. Goudie, N. J. Middleton, *Earth Sci. Rev.* **56**, 179 (2001).
8. J. M. Prospero, P. J. Lamb, *Science* **302**, 1024 (2003).
9. S. Engelstaedter, I. Tegen, R. Washington, *Earth Sci. Rev.* **79**, 73 (2006).
10. Y. J. Kaufman, D. Tanre, O. Boucher, *Nature* **419**, 215 (2002).
11. E. A. Shinn *et al.*, *Geophys. Res. Lett.* **27**, 3029 (2000).
12. T. D. Jickells *et al.*, *Science* **308**, 67 (2005).
13. I. Koren *et al.*, *Environ. Res. Lett.* **1**, 10.1088/1748-9326/1/1/014005 (2006).
14. P. Hoelzmann *et al.*, in *Past Climate Variability Through Europe and Africa*, R. W. Battarbee, F. Gasse, C. E. Stickley, Eds. (Kluwer, Dordrecht, Netherlands, 2004), pp. 219–256.
15. J. E. Kutzbach, B. L. Otto-Bliesner, *J. Atmos. Sci.* **39**, 1177 (1982).
16. S. Joussaume *et al.*, *Geophys. Res. Lett.* **26**, 859 (1999).
17. V. Brovkin, M. Claussen, V. Petoukhov, A. Ganopolski, *J. Geophys. Res. Atmos.* **103**, 31613 (1998).
18. M. Claussen *et al.*, *Geophys. Res. Lett.* **26**, 2037 (1999).
19. H. Renssen, V. Brovkin, T. Fichefet, H. Goosse, *Quat. Int.* **150**, 95 (2006).
20. Z. Y. Liu *et al.*, *Quat. Sci. Rev* **26**, 1818 (2007).
21. J. Adkins, P. Demenocal, G. Eshel, *Paleoceanography* **21**, PA4203 10.1029/2005PA001200 (2006).
22. R. B. Alley *et al.*, *Science* **299**, 2005 (2003).
23. J. A. Rial *et al.*, *Clim. Change* **65**, 11 (2004).
24. M. Scheffer, S. Carpenter, J. A. Foley, C. Folke, B. Walker, *Nature* **413**, 591 (2001).
25. J. A. Foley, M. T. Coe, M. Scheffer, G. L. Wang, *Ecosystems (N.Y., Print)* **6**, 524 (2003).
26. International Atomic Energy Agency, Report RAF/8/036 (IAEA, Vienna, 2007).
27. Materials and methods are available as supporting material on *Science* Online.
28. R. Capot-Rey, *Mém. Inst. Rech. Sahar.* **5**, 65 (1961).
29. F. White, *The Vegetation of Africa* (UNESCO, Paris, 1983).
30. R. Washington, M. Todd, N. J. Middleton, A. S. Goudie, *Ann. Assoc. Am. Geogr.* **93**, 297 (2003).
31. J. Maley, *Global Planet. Change* **26**, 121 (2000).
32. R. Washington *et al.*, *Geophys. Res. Lett.* **33**, L09401 (2006).
33. M. Maslin, *Science* **306**, 2197 (2004).
34. M. Sankaran *et al.*, *Nature* **438**, 846 (2005).
35. S. C. Dekker, M. Rietkerk, M. F. P. Bierken, *Glob. Change Biol.* **13**, 671 (2007).
36. J. van de Koppel, M. Rietker, F. J. Weissing, *Trends Ecol. Evol.* **12**, 352 (1997).
37. S. Kefi *et al.*, *Nature* **449**, 213 (2007).
38. R. Kuper, S. Kröpelin, *Science* **313**, 803 (2006).
39. U. Salzmann, P. Hoelzmann, I. Morczinek, *Quat. Res.* **58**, 73 (2002).
40. M. P. Waller, F. A. Street-Perrott, H. Wang, *J. Biogeogr.* **34**, 1575 (2007).
41. G. H. Haug, K. A. Hughen, D. M. Sigman, L. C. Peterson, U. Rohl, *Science* **293**, 1304 (2001).
42. D. Fleitmann *et al.*, *Science* **300**, 1737 (2003).
43. Y. J. Wang *et al.*, *Science* **308**, 854 (2005).
44. A. Berger, M. F. Loutre, *Quat. Sci. Rev.* **10**, 297 (1991).

45. This research was sponsored by the Deutsche Forschungsgemeinschaft through SFB 389 (ACACIA), the Research Foundation of Flanders (FWO-Vlaanderen, Belgium) and the Centre National de la Recherche Scientifique (France). We thank B. Mallaye of the Centre National d'Appui à la Recherche of Chad for research permission; U. George for support of test coring in 1999; U. Karstens, A. Noren, A. Alcantara, J. F. Crémer, G. Kabihogo, K. Van Damme, A. Myrbo, and M. Blaauw for assistance with data collection, processing, and analysis; and M. Claussen, D. Fleitmann, H. Goosse, Z. Liu, M. Maslin, J.-B. Stuut, and J. van de Koppel for discussion. Cores were logged and archived at the National Lacustrine Core Repository, University of Minnesota, Minneapolis, USA.

Supporting Online Material

www.sciencemag.org/cgi/content/full/320/5877/765/DC1
Materials and Methods
SOM Text
Figs. S1 to S4
Tables S1 and S2
References

7 January 2008; accepted 20 March 2008
10.1126/science.1154913

Supporting Online Material for

Climate-Driven Ecosystem Succession in the Sahara: The Past 6000 Years

S. Kröpelin,* D. Verschuren, A.-M. Lézine, H. Eggermont, C. Cocquyt, P. Francus, J.-P. Cazet, M. Fagot, B. Rumes, J. M. Russell, F. Darius, D. J. Conley, M. Schuster, H. von Suchodoletz, D. R. Engstrom

*To whom correspondence should be addressed. E-mail: s.kroe@uni-koeln.de

Published 9 May 2008, *Science* **320**, 765 (2008)
DOI: 10.1126/science.1154913

This PDF file includes:

Materials and Methods

1. Lake Yoa almost certainly contains a complete sequence of Holocene environmental change (*S1*); only the mid- and late-Holocene portion could be recovered with light-weight coring equipment (*S2*) operated with casing in 24.3 m water depth. The sampled sediments (composite core OUNIK03/04; 7.47 m long) are finely laminated clayey to sandy muds with 5-20% organic matter, 5-25% carbonate, and 1-13% diatom silica. In the lower half of the core (7.47-4.25 m), lamination couplets are composed of a dark brown to black organic lamina and a white lamina of endogenic calcite, occasionally supplemented by a thin red-brown lamina of wind-blown silt (Fig. 2D). In the upper half of the core (4.25-0.00 m) the red-brown laminae are thicker (4-18 mm), more frequent, and grade into the organic laminae. Above 1.57 m, almost all carbonate is detrital, and embedded within the red-brown laminae.

2. Sediment chronology was established using the ^{137}Cs-inferred time marker of nuclear bomb testing in 1963-1964 (*S3*), and 17 accelerator mass spectrometry (AMS) ^{14}C dates on charred grass, fragments of *Typha* rhizome, or bulk organic matter. A count of 39 lamination couplets above the AD 1964 $\pm$ 3 yr ^{137}Cs peak supports their classification as varves. Paired ^{14}C dates on *Typha* rhizomes and bulk organic matter yield similar results (Table S1), indicating that most carbon uptake in the root system of these stands is from the water. Our calendar age-depth model (Fig. S1) is a 3rd-order polynomial regression of INTCAL04-calibrated ^{14}C ages (*S4*) vs. cumulative dry weight down-core, after removal of three outliers and subtraction of the modern lake-carbon reservoir age from all bulk organic and *Typha* rhizome ages. This modern lake-carbon reservoir correction (1467 $\pm$ 44 ^{14}C years) is the mean ^{14}C age difference (n = 3) between two pairs of ^{14}C dates on terrestrial and aquatic organic matter, and between the uppermost ^{14}C date on bulk organic matter and its corresponding varve count (Table S1). Given dating uncertainty resulting from analytical and age-modeling error (mean $\pm$ 40 ^{14}C years and $\pm$ 70 calendar years, respectively), all calendar ages given in the text are rounded to the nearest 100 years. Preliminary varve counts on the whole sequence duplicate the ^{14}C chronology within the error range of both techniques.

3. Fossil diatom sample processing followed refs. *S5*-*S6*. Changes through time in the fossil diatom assemblage were identified using stratigraphically constrained sum-of-squares cluster analysis (CONISS; *S7*) applied to squared-root transformed species percentage data. The statistical significance of this zonation was assessed following refs. *S8*-*S9*, using ZONE 1.2 (*S10*) and BSTICK 1.0 (*S11*). Biostratigraphic diagrams were produced in TILIA 2.0.b.4. (*S12*) and TGView 2.0.2 (*S13*). Reconstructed paleosalinity (as conductivity, in µS/cm) is the weighted mean value of 5 lakes with modern diatom species composition most similar to the fossil Lake Yoa assemblage (weighted modern-analogue technique, WMAT). We used a calibration dataset containing 264 samples from ~150 African waters (*S14*) supplemented by 20 samples from 9 waters in the Ounianga region. This transfer function has an r^2_{jack} between inferred and observed log-transformed conductivity of 0.76, and a root-mean-square error of prediction (RMSEP) of 0.44 $\log_{10}$ conductivity units. All 94 fossil assemblages found good modern analogues (*S15*) in the calibration data set. Sample-specific errors (*S16*) range from 0.48-0.59 $\log_{10}$ conductivity units in the freshwater lake phase to 0.46-0.66 $\log_{10}$ conductivity units in the hypersaline lake

phase (Fig. 2A). Salinity inferences, analogue statistics and sample-specific errors were obtained in C2 1.3.4. (*S17*).

4. Aquatic invertebrate fauna analysed include the Chironomidae, Chaoboridae and Ephydridae (all Insecta Diptera), Corixidae (Insecta Hemiptera), and Chydoridae (Crustacea Anomopoda). Chaoboridae (phantom midges) and Corixidae (waterboatmen) are planktonic organisms. Ephydridae (brine flies) are in Lake Yoa restricted to sandy shoreline habitat. Chironomidae (non-biting midges) and Chydoridae (water fleas *partim*) are benthic, and in this stratified lake restricted to oxygenated shallow-water bottom habitat. Given the stable sedimentation dynamics, taphonomy and preservation of these chitinous invertebrate remains can be assumed constant throughout the studied sequence. Sample processing followed refs. *S18-S19*. Identification was done at 100 to 400-fold magnification using guides for sub-Saharan Africa (*S20-S24*). Counting criteria for fragmentary fossils followed ref. *S18*, and sample volumes were adjusted to yield the diversity-dependent fossil sum required for robust numerical analysis (*S25-S26*). Chironomid-based salinity inference is based on WMAT applied to an African calibration dataset of chironomid community composition in 87 lakes (72 in East Africa, 8 in West Africa, 7 from within the Sahara; *S27*). This transfer function has an r^2_{jack} between inferred and observed log-transformed conductivity of 0.77, and a RMSEP of 0.40 $\log_{10}$ conductivity units. On average 96 % of the fossil chironomid sum in individual samples were taxa represented in the calibration dataset; the remainder (e.g., *Chironomus* indet. sp.) are almost certainly Eurasian chironomid species with undocumented salinity tolerance (*S27*). Excluding these taxa, all 93 fossil assemblages found good modern analogues (*S15*) in the calibration data set. Sample-specific errors (*S16*) range from 0.48-0.66 $\log_{10}$ conductivity units in the freshwater lake phase to 0.42-0.48 $\log_{10}$ conductivity units in the hypersaline lake phase.

5. Pollen samples were processed according to standard procedures (*S28*) including treatment with HCL and HF, and sieving through 5 µm mesh. Addition of a known amount of exotic pollen (*Alnus*) allowed calculation of pollen concentrations (grains per ml) and fluxes (grains per cm^2 per year). In total 163 different pollen types were identified for a mean pollen sum of 406 (range 88-848) counted plant pollen and fern spores per sample. The recovered plant taxa represent the modern Mediterranean, Saharan, Sahelian, Sudanian and Tibesti-montane phytogeographical zones. Mediterranean plant taxa in Fig. 2 are mainly *Olea*, *Quercus* and *Pistacia*; Saharan plant taxa are mainly the trees *Salvadora persica* and *Ephedra*, and herbs *Artemisia*, *Cornulaca* and Amaranthaceae-Chenopodiaceae; tropical (Sudanian) plant taxa are mainly the trees *Piliostigma*, *Lannea* and *Fluggea virosa*, and herbs *Mitracarpus* and *Spermacoce*. Pollen slides also contained diagnostic remains of phytoplankton species. These could be attributed to 23 taxa of Chlorophyta (green algae), 2 taxa of Cyanobacteria (blue-green algae), and 1 taxon of Dinophyta (dinoflagellates); see Table S2.

6. Low-field magnetic susceptibility was measured on a Geotek multisensor core logger at 1 cm resolution, using a Bartington MS2E point sensor. Data are presented as mass-specific magnetic susceptibility (χ) with organic and carbonate content subtracted from total dry mass. Magnetic susceptibility measures the concentration of magnetic particles in sediments, proportional to total allochtonous mineral matter in lakes and to the relative concentration of different magnetic minerals present in the source deposit of this allochtonous matter (*S29*). Which iron-bearing mineral is primarily responsible for the magnetic properties of the sediment depends on the history of weathering regimes in the source region. In lake Yoa today, allochtonous mineral

matter is mainly the wind-blown silt that accumulates in the thin red-brown lamina, and is enriched in Fe-rich minerals. The warm and dry climate conditions which during the late Quaternary most commonly prevailed in its source region (the Ounianga area and southern Libya to the northeast) favour the formation of hematite through secondary alteration of goethite present in soils and iron crusts (*S30-31*).

Supporting online text

1. ***Lack of continuous records of Saharan climate and ecosystem change.*** The now numerous available Holocene paleolake records from the arid and subarid belts of North Africa (for a recent synthesis see ref. *S32*) document a fairly consistent scheme of an early-Holocene moist and green Sahara followed by general aridification, but pronounced differences in the apparent timing and amplitude of hydrological change inferred from individual records point to both regional variability in climate change and site-specific topographic or hydrogeological influences on reconstructed water-balance evolution (*S33*-*S34*). In addition the ubiquitous temporal hiatuses in Saharan lake-sediment archives due to desiccation, and any changes in sediment accumulation that are inadequately constrained chronologically, cryptically over-accentuate directional trends in the paleohydrological proxies (*S35*), thereby compromising inferences of the rates of climate or ecosystem change. Consequently, inferences of abrupt mid-Holocene drying (e.g., *S36*) or of fluctuations between moist and dry episodes (e.g., *S37*-*S38*) based on such individual records are difficult to substantiate, and analysis of possible regional synchrony of climate events is problematic (*S33*). At the same time, poor age control on individual records and the site-specific relationship between local water balance and climate cause supra-regional summaries of Saharan lake status through time (*S39*) to suggest more gradual climate change than may actually have occurred, besides obscuring the well-established north-south gradient in the timing of Holocene aridification over North Africa (*S34, S40*). These problems explain the attractiveness of a proxy record of Saharan climate and ecosystem change extracted from marine sediments (*S41*), a paleoenvironmental archive that is generally trusted to accumulate continuously and to faithfully monitor an areally integrated rate of change in the moisture balance on nearby continents. However, also in this record the inferred rate of terrestrial ecosystem change is affected by major variation in sediment accumulation (*S42*). Further, there is continued uncertainty about the size and location of the Saharan source region (formerly) supplying dust to that particular area of the tropical Atlantic Ocean (*S43*). Thus, only a demonstrably continuous and adequately-dated paleoenvironmental record from within the desert, such as the Lake Yoa record presented here, can reveal the true rate and trajectory of terrestrial ecosystem change associated with the Holocene desiccation of the Sahara.

2. ***Modern climatology and vegetation of the Ounianga region***. Monthly mean day- and night-time temperatures at Ounianga Kebir vary 26-42 °C and 15-26 °C during the year. Annual rainfall is erratic, ranging 0-21 mm between 1953 and 1967 (mean 3.9 mm; n = 15). Summer monsoon rainfall from the south does not occur regularly within ~300 km of the area, and wintertime depressions from the Mediterranean only occasionally reach the Tibesti, 400 km to the northwest. Monthly pan evaporation was measured at Faya Largeau (200 km to the southwest) from 1987 to 2002 (n = 16) but many values are missing. Mean annual evaporation derived from three complete annual data sets (1989, 1993, 1999) is 6330 mm; the sum of mean values available for each month (n = 9-14) is 6110 mm (weather data courtesy of the Direction des Ressources en Eau et de la Météorologie, N'Djamena, Chad). Vegetation surrounding Lake Yoa is of desert type, with plants confined to dry river beds (*S44*) except date palm (*Phoenix*), cattail (*Typha*) and some *Acacia* growing near the lakeshore.

3. ***Ecological succession in the Lake Yoa phytoplankton community***. Before 5600 cal yr BP the algal flora was characterized by the green algae *Botryococcus*, *Spirogyra* and Hydrodyctiaceae

(Fig. S2) and the diatoms *Aulacoseira*, *Chaetoceros* and *Urosolenia* (Fig. S3). After that time *Aulacoseira* and *Synedra* became the most prominent diatoms (Fig. S3); among green algae, *Botryococcus* and *Spirogyra* were replaced by Desmidiaceae (*Cosmarium, Staurastrum*) and Scenedesmaceae (*Scenedesmus*, *Coelastrum*), which reached peak abundances ~5500-5200 cal yr BP. These and other green algae almost disappeared ~4900-4800 cal yr BP, when diatom production (% biogenic SiO_2; Fig. 2B) again increased together with a slight rise in diatom-inferred lake-water salinity from 300 µS/cm to ~600 µS/cm (Fig. 2A). Inference of rising salinity reflects the appearance of salt-tolerant diatoms (*Nitzschia fonticola, N.* cf. *elliptica, Rhopalodia gibberula, Stauroneis*) at the expense of *Aulacoseira* (Fig. S3). The transition of Lake Yoa from a fresh to salt-lake environment between 4200 and 3900 cal yr BP is marked in the fossil diatom record by complete collapse of the formerly dominant *Aulacoseira* population. This benefited the salt-tolerant species already present, and newly appearing salt-loving taxa (Fig. S3: *Anomoeoneis sphaerophora, Nitzschia frustulum*). Paleoecological interpretation and salinity inference based on the fossil diatom record after 3900 cal yr BP is complicated by the presence of taxa with unknown ecological affinity, and by contamination of the local salt-lake species assemblages with freshwater taxa eroded from early-Holocene diatomites exposed nearby. Incongruent freshwater diatom assemblages containing *Aulacoseira, Synedra* and *Campylodiscus* continue to be deposited in Lake Yoa today, and even dominate the fossil record since 2700 cal yr BP because autochtonous diatom production in this hypersaline environment has been virtually non-existent (Fig. 2B: ~3% biogenic SiO_2; Fig. S2: on average 0.13×10^6 diatom frustules per mg dry sediment). After correcting for these known complicating factors, the diatom-inferred conductivity for Lake Yoa has a rather stable mean value of ~10,000 µS/cm for the past ~3600 years, still significantly below the observed modern value of 69,000 µS/cm. We attribute this difference mainly to the lack of hypersaline calibration lakes with diatom flora similar to that of the modern Lake Yoa.

4. ***Ecological succession in the Lake Yoa zooplankton and zoobenthos***. The stratigraphic distribution of aquatic insects and microcrustaceans (Figs. S2, S4) confirms that until 4800 cal yr BP Lake Yoa was a deep and dilute freshwater environment with diverse nearshore habitat including submerged vegetation. Impact of evaporative concentration on the osmotic balance of these aquatic plants is indicated from 4800 cal yr BP by reduction in *Polypedilum* nr. *deletum* and vegetation-dwelling Chydoridae (*S45*). Secondary productivity of Lake Yoa (as indicated by fossil chironomid abundance; Fig. S4) peaked during the fresh-to-saline transition at 4200-3900 cal yr BP. It started to decrease when conductivity rose above the critical physiological threshold of 3000 µS/cm (*S46-S47*), and virtually all salt-intolerant freshwater zoobenthos were eradicated. In the meso- to hypersaline environment prevailing after that time, secondary productivity stabilised at ~30% of the mean value attained during the freshwater phase. The transition to a true salt-lake community at 3400 cal yr BP is indicated by the disappearance of all remaining Chydoridae, *Chaoborus,* and freshwater Chironomidae (*Dicrotendipes* cf. *kribiicola, Cladotanytarsus pseudomancus*).

5. Quality of the Lake Yoa record as paleoenvironmental archive. The continuously laminated deposits recovered from Lake Yoa testify that, notwithstanding its evolution from a fresh to hypersaline ecosystem, the water-column and sedimentation processes which control its incorporation of climate proxies and ecological indicators in the sediment record have remained constant throughout the last 6000 years. Furthermore the almost linear age-depth relationship (r^2 of age versus depth = 0.982; r^2 of age versus cumulative dry weight = 0.985; n = 14) indicates

that the rate of profundal sediment accumulation has been near-constant through time. Therefore, absolute concentrations of sediment components (organic matter, biogenic SiO_2, sand) and the fossils contained in them approximate their true rate (flux) of offshore deposition through time. For example, since organic matter preservation and its dilution by mineral sediments has remained more or less unchanged, the principal trends in % organic matter through time can be treated as reflecting change in aquatic primary production.

6. ***Proxy indicators of wind strength.*** We hypothesize that in the currently hypersaline lake, dune sand is transported to the mid-lake coring site mostly by saltation from a nearby dune into the lake followed by entrapment in a soapy film at the water surface. Thus, sand content of offshore sediments is primarily a function of dune size and proximity. For example, coincidence of a reduction in *Typha* pollen since ~1700 cal yr BP with sand values rising to > 20% of the dry sediment indicate that expanding dunes encroached upon suitable *Typha* habitat along Lake Yoa's northern shore (cf. Fig. 1C). Background values of 1-5% fine sand in the lower part of the record can be attributed to surface runoff and/or river input from a vegetated landscape. Availability of larger quantities of sand to start building lakeshore dunes from 3700 cal yr BP evidently also reflects the increasing mobilization of sand following regional loss of vegetation cover, but the direct relationship of profundal sand content with climatic drought or wind strength is unclear. In contrast, total fine-grained aeolian input (reflected in sediment magnetic susceptibility; see *S31*) is proportional to the fraction of the landscape lacking vegetation cover, as long as the supply of loose soil weathered during previous wetter periods is unlimited. Our combined evidence indicates that in northern Chad this was the case between 4300 and 2700 cal yr BP. Stable background values of magnetic susceptibility before 4300 cal yr BP are consistent with palynological evidence that regional vegetation cover (mostly grassland) was close to 100%. The spike in magnetic susceptibility at ~4200 cal yr BP may indicate that the earliest vegetation loss was relatively abrupt, or alternatively that early dust storms were infrequent high-volume events. After 2700 cal yr BP, mineral dust flux became limited by the rate of new erosion of suitable sediments and rocks in the now mostly barren landscape. Total pollen influx (and after 4000 cal yr BP grass pollen influx) is mainly a function of wind strength and remaining grass cover. Trade-wind direction in the region has not changed since the early Holocene (*S48-S49*), due to topographic control of the Tibesti-Ennedi corridor.

7. ***Incongruent occurrence of pollen taxa***. Scattered occurrences of tropical pollen types in the upper part of the sequence (after 2700 cal yr BP) were probably eroded from early-Holocene lake deposits nearby. An olive species endemic to the Saharan mountains, *Olea laperrini*, dominated mid-Holocene vegetation at ~2150 m in the Ahaggar massive (*S50*). Given its complete absence in the contemporaneous core interval at Lake Yoa, this species is unlikely to be the source of *Olea* pollen deposited in Lake Yoa after 2500 cal yr BP.

8. ***Evidence for mid-Holocene climatic fluctuations.*** Some vegetation (*S37*) and hydrological (*S38, S51-S52*) records as well as regional compilations of ^{14}C dates on lacustrine deposits (*S53*) suggest that the mid-Holocene drying of the Sahara proceeded as a series of multi-decadal or century-scale fluctuations between moist and dry episodes superimposed on the long-term drying trend. Such rapid climate and ecosystem swings are also produced by model simulations incorporating decade-scale climate variability (*S39, S54-S55*). The Lake Yoa record shows marked cyclic variation in pollen influx at ~600-year intervals between 6000 and 4300 cal yr BP (Fig. 2G), with the timing of influx minima (at 5800-5600 and 5100-4800 cal yr BP) broadly

matching the timing of drought spells inferred from a tree-ring record in southwestern Libya (*S52*). However, influx rates of all major terrestrial pollen types (grasses, *Acacia*, tropical plant taxa, *Erica* type *arborea*) are affected in near-equal fashion, and pollen percentage data (e.g., % grasses: Fig. 2G) show a gradual decline throughout this period. We therefore ascribe the century-scale pollen influx fluctuations to variation in the proportion of air- and river-borne pollen input to Lake Yoa, rather than to real shifts in the regional vegetation ecotone. Thus, pollen influx maxima at 6100-5900, 5500-5200, and 4900-4700 cal yr BP represent climatically wet episodes when enhanced discharge of a possibly seasonal river (wadi) into Lake Yoa brought a greater proportion of pollen types from higher (and naturally wetter) areas on the eastern slopes of the Tibesti. We envision that such century-scale rainfall fluctuations between 6000 and 4300 cal yr BP had sufficient amplitude to affect highland tree growth (*S52)* and elicit a marked hydrological response in some Saharan lakes that were isolated from the regional groundwater table, but not in the groundwater-buffered Lake Yoa. More importantly, these rainfall fluctuations did not measurably interrupt the gradual southward retreat of vegetation ecotones during the mid-Holocene. In the aquatic ecosystem indicators, we observe 1) a diatom-inferred temporary decrease of Lake Yoa conductivity to ~4000 µS/cm around 2300 cal yr BP after having attained >10,000 µS/cm in the period 3800-2600 cal yr BP; and 2) a chironomid-inferred decrease to ~20,000 µS/cm in much of the period 2100-1200 cal yr BP, from values >25,000 µS/cm in the period 3400-2400 cal yr BP. Since both of these inferred salinity reversals depend on abundance changes in just one or a few species of aquatic biota, remain within method- and sample-specific uncertainty ranges, and are not reproduced in other hydrological indicators, we consider the evidence for significant fluctuations in lake water balance during those late-Holocene episodes to be weak.

9. ***Inferences of total annual rainfall.*** Our data are qualitatively consistent with the gradual decrease from 6000 cal yr BP of monsoon precipitation in the sector 18-23°N / 11-34°E (which includes the Ounianga region) that is simulated in a synchronously coupled ocean-atmosphere-terrestrial ecosystem GCM (*S39*). Quantitatively our pollen data indicate a slightly lower annual total of ~250 mm at 6000 cal yr BP (allowing tropical savannah with 10-15% tree cover; *S56*) than the 400 mm simulated in ref. *S39*, and values of < 150 mm by 4300 cal yr BP and < 50 mm by 2700 cal yr BP. Total annual precipitation required to support savanna vegetation at 20° N latitude is estimated to lie between 180 and 260 mm (*S57-S59*). However, ecohydrological modeling indicates that the intermittent rainfall regime and large inter-annual climate variability typical of desert fringe ecosystems may allow vegetation persistence at significantly lower values of total annual rainfall (*S60*). Integration of archaeological, geological, archaeozoological and archaeobotanical data across the eastern Sahara (*S40*) inferred annual rainfall in the Ounianga region to have fallen to below 150 mm by 3500 cal yr BP.

Supplementary tables

Table S1. Radiometric (^{137}Cs, ^{14}C) dates obtained on Lake Yoa composite core OUNIK03/04.

Comp. Depth	Cumul. Dry Wt	Dated Material	Lab No.	^{14}C Age	Error	Corr. ^{14}C Age	Cal yr BP	2 σ range
cm blf	g/cm^2			years BP	+/- SD	years BP		
7.0	3.820	137Cs peak	SMM				AD 1963	
16.0	8.145	varve count					AD 1918	
16.0	8.145	*Typha* rhizome	Poz-8729	1380	30	-80		
35.0	19.175	bulk organic matter	Poz-8739	*2160*	*35*	*693*	*640*	*553-726*
35.0	19.175	*Typha* rhizome	Poz-8730	1900	50	433	430	310-550
36.0	19.797	grass charcoal	Poz-8731	315	30	315	384	304-464
59.0	34.091	*Typha* rhizome	Poz-8733	1675	30	208	210	0-421
75.0	43.577	*Typha* rhizome	Poz-8734	2200	100	733	718	544-891
79.0	45.949	bulk organic matter	Poz-8738	*2905*	*30*	*1438*	*1389*	*1272-1506*
79.0	45.949	*Typha* rhizome	Poz-8735	2020	40	553	581	509-653
87.0	51.011	grass charcoal	Poz-8736	670	30	670	618	560-675
89.0	52.339	bulk organic matter	Poz-5065	2225	30	758	676	567-786
118.5	68.782	bulk organic matter	Poz-5122	1930	30	463	476	324-628
289.5	171.954	bulk organic matter	Poz-5066	3460	40	1993	1966	1825-2106
367.5	228.389	bulk organic matter	Poz-5067	3695	35	2228	2232	2116-2347
403.5	252.715	bulk organic matter	GrA-32023	*6535*	*40*	*5068r*	*5790*	*5662-5919*
495.5	301.820	bulk organic matter	GrA-32258	5065	35	3598	3903	3729-4077
583.5	336.751	bulk organic matter	GrA-32086	5725	40	4258	4794	4628-4959
729.5	406.901	bulk organic matter	GrA-32027	6420	40	4953	5739	5589-5889
747.0	415.219						6096	5907-6185

blf: below lake floor; Corr. ^{14}C Age: after subtraction of the estimated lake-carbon reservoir age of 1467 $\pm$ 44 ^{14}C years (mean of three estimations; see Methods); SMM: Science Museum of Minnesota; Poz: Poznań Radiocarbon Laboratory; GrA: Rijksuniversiteit Groningen Radiocarbon Laboratory. Three outlying dates on bulk organic matter are indicated in italics.

Table S2. List of non-diatom phytoplankton taxa with diagnostic micro-remains recovered from Lake Yoa composite core OUNIK03/04.

Chlorophyta
Chlorococcales
- Chlorococcaceae: *Tetraedron*
- Dictyosphaeriaceae: *Botryococcus*
- Hydrodictyaceae: *Pediastrum* (8 species), *Sorastrum*
- Scenedesmaceae: *Coelastrum*, *Scenedesmus*

Desmidiales
- Desmidiaceae: *Cosmarium* (2 species), *Euastrum*, *Staurastrum*

Zygnematales
- Zygnemataceae: *Spirogyra*

Colony-building coccoids
- Oocystaceae: *Chlorella*

Cyanobacteria
Chroococcales
- Chroococcaceae: *Chroococcus*, *Gloeotrichia*

Dinophyta
- Dinophyceae: *Ceratium*

Supplementary figures

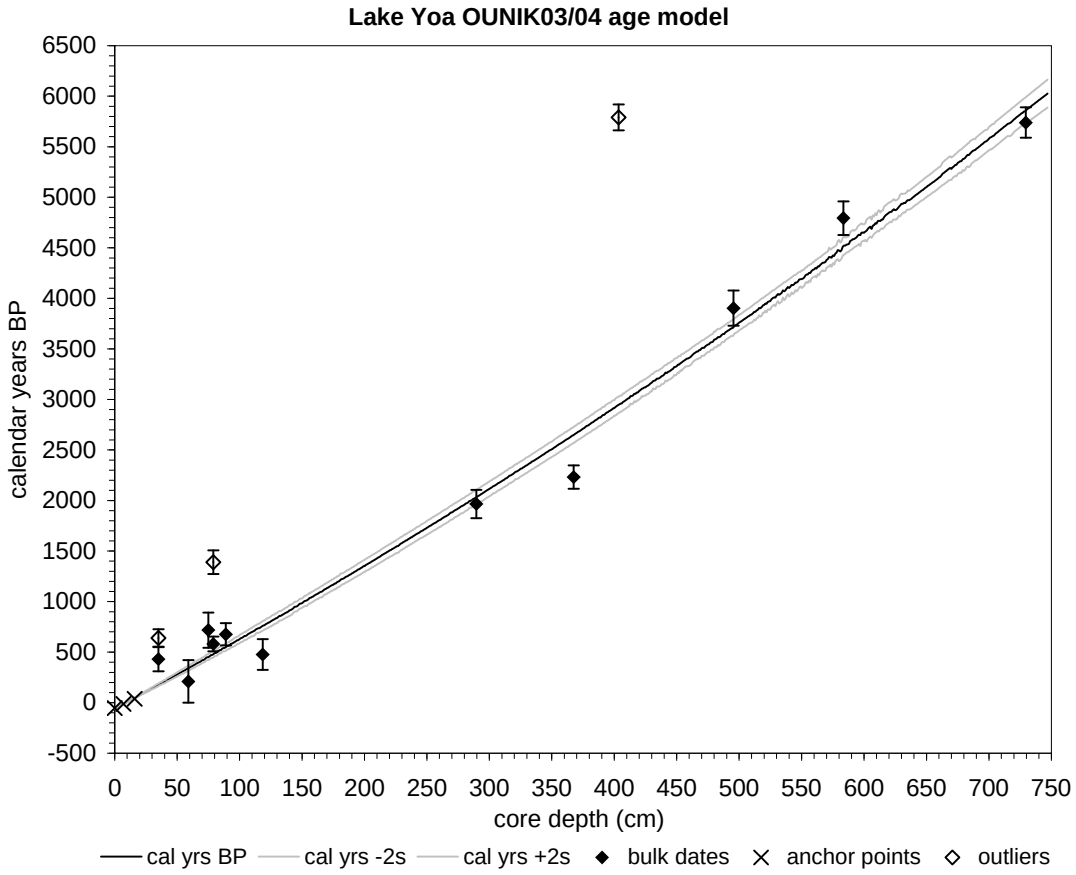

Fig. S1. Age-depth relationship of composite core OUNIK03/04 from Lake Yoa, based on a 3rd-order polynomial regression of 3 anchor points and 12 INTCAL04-calibrated ^{14}C ages vs. cumulative dry weight down-core; see Methods section 2.

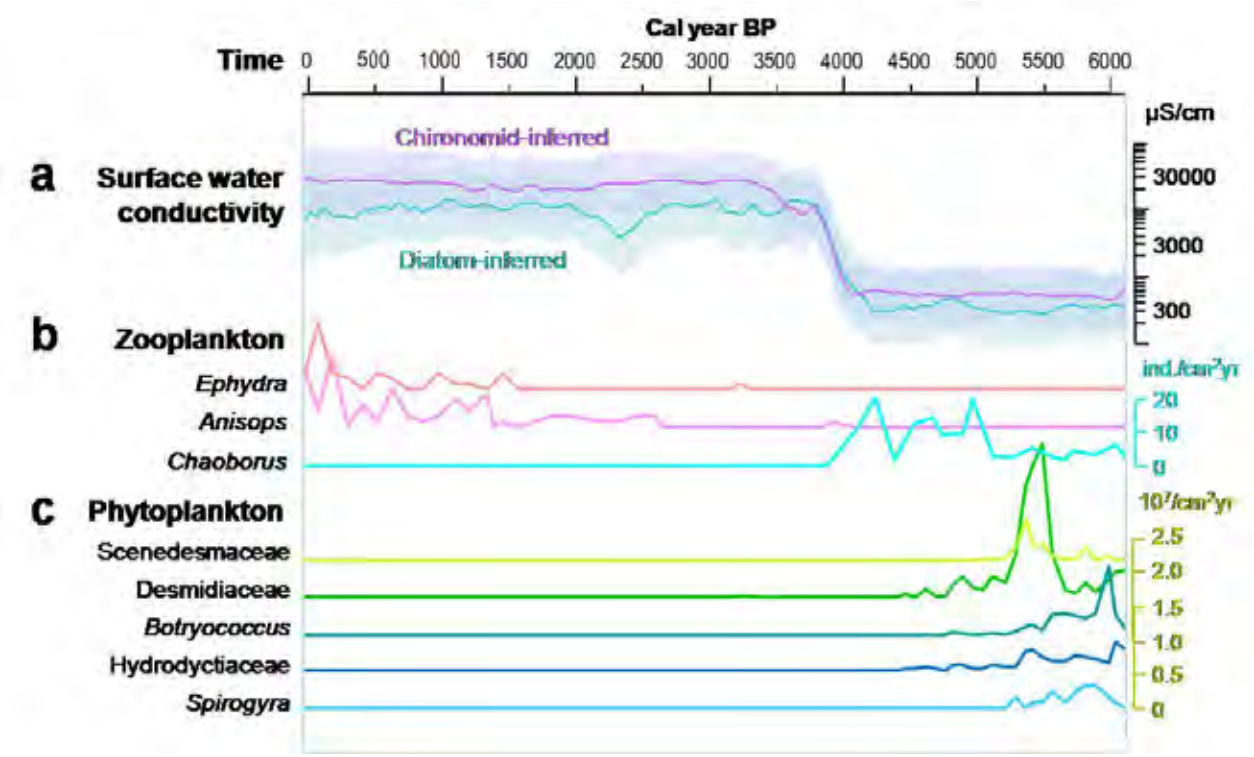

Fig. S2. Evolution of selected zooplankton and phytoplankton taxa in Lake Yoa over the past 6000 years.

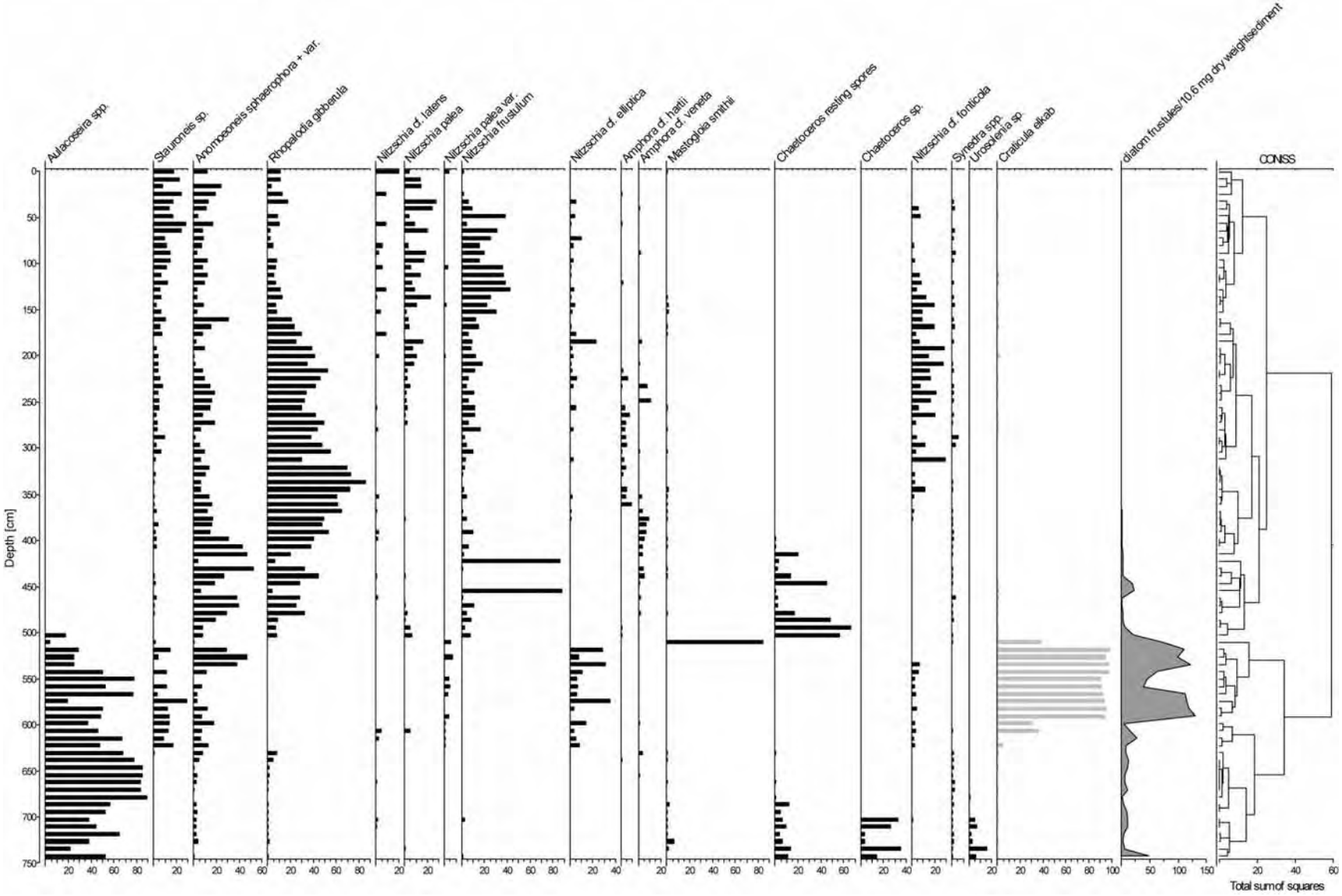

Fig. S3. Stratigraphic distribution of fossil diatom taxa [%] in composite core OUNIK03/04 from Lake Yoa, northern Chad. Biostratigraphic zonation is based on CONISS (Grimm 1987).

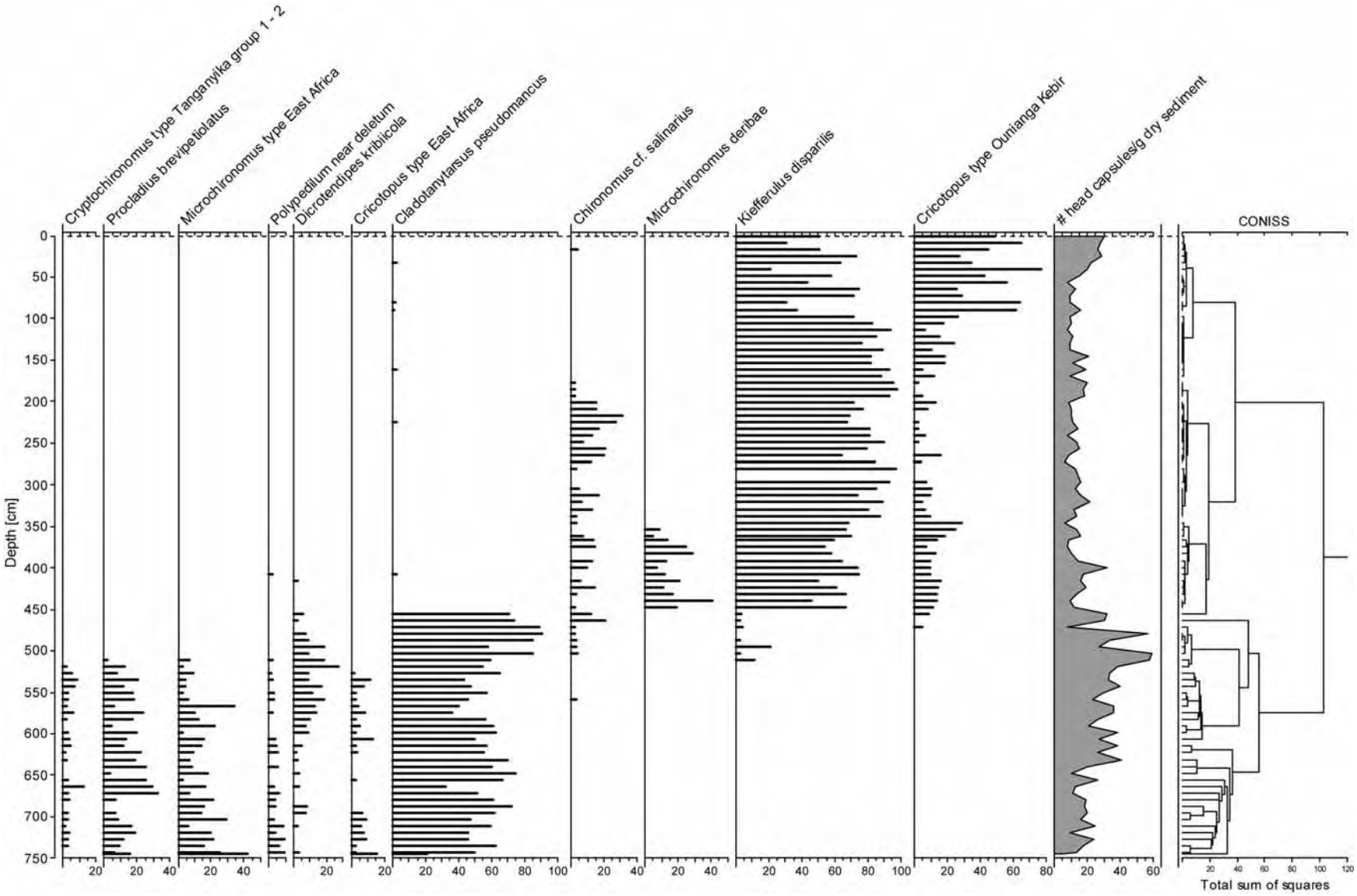

Fig. S4. Stratigraphic distribution of fossil chironomid taxa [%] in composite core OUNIK03/04 from Lake Yoa, northern Chad. Biostratigraphic zonation is based on CONISS (Grimm 1987).

Supplementary references

S1. S. Kröpelin, in *Atlas of Cultural and Environmental Change in Arid Africa*, O. Bubenzer, A. Bolten, F. Darius, Eds. (Heinrich-Barth-Institut, Köln, Germany, 2007), pp. 54-57.
S2. H. E. Wright, *J. Sediment. Petrol.* **37,** 975 (1967).
S3. P. G. Appleby, in *Tracking Environmental Change Using Lake Sediments: Basin Analysis, Coring, and Chronological Techniques*, W. M. Last, J. P. Smol, Eds. (Kluwer Academic Publishers, Dordrecht, The Netherlands, 2001), pp. 171-203.
S4. P. J. Reimer *et al.*, *Radiocarbon* **46**, 1029 (2004).
S5. H. J. Schrader, *Nova Hedwigia* **45**, 403 (1973).
S6. C. Cocquyt, D. Schram, *Hydrobiologia* **436**, 59 (2000).
S7. E. C. Grimm, *Comput. Geosci.* **13**, 13 (1987).
S8. H. J. B. Birks, A. D. Gordon, Eds., *Numerical methods in Quaternary pollen analysis* (Academic Press, 1985) pp. 317.
S9. K. D. Bennett, *New Phytol.* **132**, 155 (1996).
S10. S. Juggins, *ZONE 1.2* (Environmental Change Research Center, University College London, London, 1991).
S11. J. M. Line, H. J. B. Birks, unpublished software.
S12. E. C. Grimm, *TILIA 2.0 version b.4* (Illinois State Museum, Research and Collection Center, Springfield, Illinois, 1993).
S13. E. C. Grimm, *TGView version 2.0.2.* (Illinois State Museum, Research and Collection Center, Springfield, Illinois, 2004).
S14. F. Gasse, S. Juggins, L. B. Khelifa, *Palaeogeogr. Palaeoclimatol. Palaeoecol.* **117,** 31 (1995).
S15. A. L. Clarke *et al.*, *Limnol. Oceanogr.* **51**, 385 (2006).
S16. H. J. B. Birks, in *Statistical Modelling of Quaternary Science Data*, D. Maddy, J. S. Brew, Eds. (Cambridge Quaternary Research Association, Cambridge, 1995), pp. 161-254.
S17. S. Juggins, *C2, user Guide; Software for Ecological and Palaeoecological Data Analysis and Visualisation.* (University of Newcastle, Newcastle upon Tyne, United Kingdom,1993).
S18. I. R. Walker, in *Tracking Environmental Change using Lake sediments: Zoological Indicators*, J. Smol, H. J. B. Birks, W. Last, Eds. (Kluwer Academic Publishers, Dordrecht, The Netherlands, 2001), Developments in Paleoenvironmental Research, vol. 4, pp. 43-66.
S19. D. Verschuren, H. Eggermont, *J. Paleolimnol.* **38**, 329 (2007).
S20. D. Verschuren, *Arch. Hydrobiol. Beih.* **107**, 467 (1997).
S21. H. Eggermont, D. Verschuren, *J. Paleolimnol.* **32**, 383 (2004a).
S22. H. Eggermont, D. Verschuren, *J. Paleolimnol.* **32**, 413 (2004b).
S23. H. Eggermont, D. Verschuren, H. J. Dumont, *J. Biogeogr.* **32**,1063 (2005).
S24. B. Rumes, H. Eggermont, D. Verschuren, *Hydrobiologia* **542**, 297 (2005).
S25. O. Heiri, A. F. Lotter, *J. Paleolimnol.* **26**, 343 (2001).
S26. R. Quinlan, J. P. Smol, *J. Paleolimnol.* **26**, 327 (2001).
S27. H. Eggermont et al., *Quat. Sci. Rev.* (submitted).
S28. K. Faegri, J. Iversen. *Textbook of pollen analysis.* (Wiley, Chicester, 1989).
S29. J. A. Dearing, in *Quaternary Climates, Environments and Magnetism*, B. A. Maher, R. Thompson, Eds. (Cambridge University Press, 1999) pp. 231-278.
S30. B. A. Maher, R. Thompson (Eds.). *Quaternary climates, environments and magnetism*. (Cambridge University Press, 1999).

S31. D. Nahon, *Palaeoecol. Afr.* **12**, 63 (1980).
S32. P. Hoelzmann *et al.*, in *Past climate variability through Europe and Africa*, R. W. Battarbee, F. Gasse, C. E. Stickley, Eds. (Kluwer, Dordrecht, Netherlands, 2004), pp. 219–256.
S33. F. Gasse, *Quat. Sci. Rev*. **21,** 737 (2002).
S34. D. Fleitmann *et al.*, *Science* **300**, 1737 (2003).
S35. D. Verschuren, *Quat. Sci. Rev*. **18,** 821 (1999).
S36. J. C. Ritchie, C. H. Eyles, C. V. Haynes, *Nature* **314,** 352 (1985).
S37. A. M. Lézine, J. Casanova, C. Hillaire-Marcel, *Geology* **18**, 264 (1990).
S38. J. Fabre & N. Petit-Maire, *Palaeogeogr. Palaeoclimatol. Palaeoecol.* **65**, 133 (1988).
S39. Z. Liu *et al.*, *Quat. Sci. Rev*. **26,** 1818 (2007).
S40. R. Kuper, S. Kröpelin, *Science* **313**, 803 (2006).
S41. P. B. deMenocal *et al.*, *Quat. Sci. Rev.* **19**, 347 (2000).
S42. J. Adkins, P. Demenocal, G. Eshel, *Paleoceanography* **21,** Art. No. PA4203 (2006).
S43. J. B. Stuut *et al.*, *J. Geophys. Res.-Atmos.* **110**, Art. No. D04202 (2005).
S44. R. Capot-Rey, *Mém. d'Institut de Recherches Sahariennes* **5** (1961).
S45. D. Verschuren, J. Tibby, K. Sabbe, N. Roberts, *Ecology* **81,** 164 (2000).
S46. D. S. Rawson, J. E. Moore, *Can. J. Res. D* **22**, 141 (1944).
S47. U. T. Hammer, *Monogr. Biol.* **59** (1986), 616 pp.
S48. S. Kröpelin, *Berliner Geogr. Abh.* **54** (1993).
S49. M. Schuster *et al.*, *Quat. Sci. Rev.* **24**, 1821 (2005).
S50. M. Thinon, A. Ballouche, M. Reille, *Holocene* **6,** 457 (1996).
S51. F. Mees, D. Verschuren, R. Nijs, H. Dumont, *J. Paleolimnol.* **5**, 227 (1991).
S52. M. Cremaschi, M. Pelfini, M. Santilli, *Holocene* **16**, 293 (2006).
S53. N. Petit-Maire, Z. Guo, S. Kröpelin, *Global Planet. Change* **26**, 97 (2000).
S54. H. Renssen, *Geophys. Res. Lett.* **30,** Art. No. 1184 (2003).
S55. H. Renssen, V. Brovki, T. Fichefet, H. Goosse, *Quatern. Int.* **150**, 95 (2006).
S56. M. Sankaran *et al*., *Nature* **438**, 846 (2005).
S57. V. Brovkin, M. Claussen, V. Petoukhov, A. Ganopolski, *J. Geophys. Res.-Atm*. **103**, 31613 (1998).
S58. S. Joussaume *et al.*. *Geophys. Res. Lett.* **26,** 859 (1999).
S59. M. Scheffer, M. Holmgren, V. Brovkin, M. Claussen, *Global Change Biol.* **11,** 1003 (2005).
S60. M. Baudena, G. Boni, L. Ferraris, J. von Hardenberg, A. Provenzale, *Adv. Water Resources* **30**, 1320 (2007).